Global Aurora on Mars during the September 2017 Space Weather Event

N.M. Schneider[1*], S.K. Jain[1], J. I. Deighan[1], C. R. Nasr[1], D.A. Brain[1], D. Larson[2], R. Lillis[2], Ali Rahmati[2], J.S. Halekas[3], C. O. Lee[2], M.S. Chaffin[1], A. Stiepen[1], M. Crismani[1], J.S. Evans[4], M.H. Stevens[5], D.Y. Lo[6], W.E. McClintock[1], A.I.F. Stewart[1], R.V. Yelle[6], J.T. Clarke[7], G.M. Holsclaw[1], F. Lefevre[8], F. Montmessin[8], and B.M. Jakosky[1]

[1]Laboratory for Atmospheric and Space Physics, University of Colorado at Boulder.

[2]Space Science Laboratory, University of California, Berkeley.

[3]Department of Physics and Astronomy, University of Iowa.

[4]Computational Physics, Inc.

[5]Space Science Division, Naval Research Laboratory.

[6]Lunar and Planetary Lab, University of Arizona.

[7]Center for Space Physics, Boston University.

[8]LATMOS/IPSL, Guyancourt, France.

*Corresponding Author: nick.schneider@lasp.colorado.edu.

Key points.

- The MAVEN spacecraft has obtained the first images of aurora on Mars.
- Mars aurora can be global in nature, due to its lack of a global magnetic field.
- The global aurora was triggered by a space weather event observed by many instruments and spacecraft.
- Mars' crustal magnetic fields influenced faint auroral emissions during the declining phase of the event.

This article has been accepted for publication and undergone full peer review but has not been through the copyediting, typesetting, pagination and proofreading process which may lead to differences between this version and the Version of Record. Please cite this article as doi: 10.1029/2018GL077772

Index Terms: 6225, 5408, 5405, 5421, 5464

Keywords: Mars, aurora, space weather, magnetic fields

Abstract. We report the detection of bright aurora spanning Mars' nightside during the space weather event occurring in September 2017. The phenomenon was similar to diffuse aurora detected previously at Mars, but 25 times brighter and detectable over the entire visible nightside. The observations were made with the Imaging UltraViolet Spectrograph (IUVS), a remote sensing instrument on the Mars Atmosphere and Volatile EvolutioN (MAVEN) spacecraft orbiting Mars. Images show that the emission was brightest around the limb of the planet, with a fairly uniform faint glow against the disk itself. Spectra identified four molecular emissions associated with aurora, and limb scans show the emission originated from an altitude of ~60 km in the atmosphere. Both are consistent with very high energy particle precipitation. The auroral brightening peaked around 13 September, when the flux of solar energetic electrons and protons both peaked. During the declining phase of the event, faint but statistically significant auroral emissions briefly appeared against the disk of the planet in the form of narrow wisps and small patches. These features are approximately aligned with predicted open field lines in the region of strong crustal magnetic fields in Mars' southern hemisphere.

1. Introduction

The MAVEN spacecraft has been orbiting Mars since 21 September 2014, with a primary mission to study the behavior of the upper atmosphere and the escape of its constituent gases to space [*Jakosky et al., 2014*]. MAVEN orbits Mars on a 4.5 hour elliptical orbit, with a closest approach to Mars' surface at periapse of 150-200 km and an apoapse around 5900 km at the time of the observations. MAVEN carries one remote sensing instrument for the study of Mars' upper atmosphere, the Imaging UltraViolet Spectrograph (IUVS) [*McClintock et al., 2015*]. The instrument captures spectra of the planet and its atmosphere in the far-UV (110-190 nm) and mid-UV (180-340 nm), ideal for recording well-known atmospheric emissions from CO_2 and its dissociation and ionization products. The instrument is mounted on an Articulated Payload Platform (APP) that can orient IUVS's field of view relative to Mars depending on spacecraft location, orientation and desired viewing geometry. IUVS was designed to observe Mars dayglow, nightglow, hydrogen corona, D/H ratio and stellar occultations, and is also sensitive to auroral emissions.

Mars exhibits at least three types of aurora. The SPICAM instrument on Mars Express discovered discrete aurora: small short-lived patches of aurora related to the crustal magnetic fields in Mars' southern hemisphere [*Bertaux et al*., 2005]. Discrete aurora have been attributed to particles accelerated to energies <1 keV by magnetic field reconfiguration at Mars, and have been primarily observed at altitudes around 140 km [*Gerard et al.*, 2015, *Brain et al.*, 2006].

MAVEN/IUVS discovered a second type called diffuse aurora [*Schneider et al.,* 2015a], with emissions spanning much of Mars' nightside for five days in December 2014. The phenomenon was observed again in March 2015 [*Jakosky et al.*, 2015], and has been seen occasionally since. Diffuse aurora are attributed to solar energetic particles (SEP's), specifically electrons accelerated to energies of ~100 keV at the Sun and heliospheric shock

fronts. MAVEN carries an instrument also abbreviated SEP dedicated to the detection of such particles [*Larsen et al.,* 2015]; hereafter we refer to it as MAVEN/SEP. Such particles can penetrate to great depths in the atmosphere, and IUVS observations yielded peak emissions altitudes in the range 60-70 km. Theoretical work by *Gerard et al*. 2018 confirmed that 100 keV electrons are capable of exciting auroral emission at 60 km altitude, but neither that work nor *Schneider et al*. [2015a] was able to demonstrate that the observed emission profile could be modelled quantitatively by emission from the precipitating electron population.

MAVEN/IUVS also discovered a third form called proton aurora occurring on Mars' dayside, caused by penetrating protons from the solar wind [*Deighan et al*. 2018, *Halekas et al.* 2017]. The MAVEN/IUVS detection of proton aurora prompted a search in the Mars Express SPICAM archive [*Ritter et al*., 2018], finding six events and confirming the existence of the phenomenon.

2. Observations

Two of IUVS's observing modes captured aurora emissions. As neither of these modes have been employed in previously published studies, we briefly describe them below.

First, IUVS obtains ultraviolet spectral images of Mars' disk during the 70 minutes surrounding apoapse. Since the spectrograph uses an entrance slit, the slit must be scanned across Mars' ~55˚ diameter disk to construct an image. Since the IUVS slit spans 11 degrees, only a narrow swath across the planet can be recorded at a time. The complete image can be constructed by taking advantage of spacecraft motion about the planet, allowing several image swaths to be taken sequentially while the spacecraft is inertially pointed. Note that the ~70 minute duration of imaging and the changing viewing geometry means that the image should not be considered a snapshot from a single location at a moment in time. Slit pointings on and near Mars' dayside use low intensifier gain to avoid saturating the detector. Nightside

pointings use high gain for optimum sensitivity to faint emissions. At each slit pointing, a spatially-resolved spectrum is taken. The detector readout is binned spatially and spectrally according to the observation's scientific goals and the limits imposed by data downlink to Earth. For these observations, a limited mid-UV spectral range 195-220 nm was recorded in 40 spectral bins, sufficient to capture and spectrally distinguish two important molecular emissions observed on Mars' nightside: CO Cameron bands observed in aurora and nitric oxide (NO) nightglow emissions. The spectra are fitted against templates for these two emissions using multiple linear regression [*Stevens et al*., 2015]. Observations are normally taken every orbit, at 4.5 hour intervals, with occasional interruptions for data downlinks to Earth. The observation files used in this work are identified as "apoapse", version 12, of the Level 1b data available on the Planetary Data System (PDS).

Second, an alternative type of limb scans was used to provide complete spectra and vertical profiles of atmospheric emissions. Previous IUVS publications [e.g., *Schneider et al*. 2015b], used limb scans obtained during MAVEN's periapse. In September 2017, MAVEN's periapse lay on Mars' dayside such that these commonly-used limb scans could not view Mars' nightside. IUVS also obtains limbs scans during the orbit side segments as the spacecraft recedes from periapse and later approaches for the next periapse. The limb tangent point in this geometry lies approximately antipodal to periapse, hence lies on Mars nightside during this period. For side segment limb scans, the IUVS slit is pointed inward toward the orbit's line of apsides, and oriented tangent to the limb. Spacecraft motion carries the inertially-pointed slit upwards or downwards across the atmosphere at the limb. Small scan mirror repointings allow multiple limb scans to be obtained during each orbit side segment. For these observations, full spectral coverage can be recorded. This adds three nightside emissions to the CO Cameron band and NO emission recorded in imaging mode: the CO_2^+ ultraviolet doublet at 289 nm, the atomic oxygen line at 297.2 nm, and the CO_2^+ Fox-

Duffendack-Barker bands between 300-340 nm. The observation files used in this work are identified as “inlimb” and “outlimb”, version 12, of the Level 1b data available at the PDS. Inlimb/outlimb pairs were obtained every four orbits due to timesharing with other observations.

3. Results

Figure 1 shows Mars nightside images taken at the start and at the peak of the space weather event, with brightness corresponding to the fitted spectrum of Cameron band emission as previously observed in Mars aurora. In the left image, Mars’ disk shows a uniform background consistent with instrument noise, and the limb shows a faint but significant brightening. In the right image taken at the peak, all parts of the nightside observed at high gain show elevated emission, i.e., aurora covers the entire observable nightside, and limb brightening of the optically thin emission is very pronounced. Auroral brightenings were observed in a total of 15 images over the 7-26 September period. Diffuse aurora, widespread across the night side, had previously been detected in limb scan observations [*Schneider et al.*, 2015a], but the observations reported here are the first images of aurora of any type on Mars.

Figure 2 shows the spectrum and altitude profiles of the emission obtained from inlimb observations obtained during Orbit 5730 near the peak of the space weather event. The prominence of the CO_2^+ ultraviolet doublet (UVD) emission compared to CO Cameron band emission is consistent with high energy excitation associated with SEP particles and diffuse aurora [*Gerard et. al.*, 2017], unlike the discrete aurora emissions dominated by CO Cameron bands. Both the spectrum and vertical profiles of Figure 2 are consistent with those reported in the discovery of diffuse aurora [*Schneider et al.*, 2015a, *Jakosky et al.* 2015] but at a

brightness about 25 times higher in September 2017 than March 2015. Significant diffuse auroral emission was detected in an additional 20 inlimb or outlimb observations over the 7-26 September period. Periapse limb scan observations of Mars' dayside were optimal for the detection of proton aurora through H Lyman alpha emission, but no occurrences were detected.

Figure 3 shows the timeline of diffuse auroral detections and precipitating particle populations. The aurora exhibit three distinct events: 11-14 September, 17-18 September, and 20-21 September. The first is more than ten times brighter than the other two. The primary auroral brightening during the first event correlates well with either MAVEN/SEP electrons or protons. The third auroral event corresponds better with MAVEN/SEP protons, but the second event has no corresponding rise in either MAVEN/SEP electrons or protons. It bears noting that MAVEN/SEP measurements are made thousands of kilometers away from the aurora themselves, so a perfect correlation is not expected. We conclude that comparison of the timelines alone does not identify a unique correlation with either MAVEN/SEP electrons or protons.

Figure 4 (top) shows an unusual phenomenon which only occurred on Orbit 5738 within this extended period. The ~hour-long observation was obtained on 14 September 2018 centered around 12:46 UTC. Wisps and patches of potential auroral emission appeared across the nightside, unlike the bright limb glow and uniform disk emission of the other fifteen apoapse images. Groups of pixels with enhanced brightness were identified by eye and given alphabetical identifiers. While the spectra associated with individual pixels have marginal signal-to-noise ratios, groups of such pixels can be co-added to compare their spectra to spectral templates for CO Cameron band emission, nitric oxide nightglow, or broadband features associated with cosmic rays or stray light occurring within the instrument. Wisps and patches whose spectra showed a good statistical match to Cameron band emission were

color-coded purple, and those with poor statistics or spectral evidence of instrumental artifacts were coded orange. Note in particular that all of the horizontal linear features (E, F, G, J, and O) proved to be instrument artifacts. This is likely due to occasional cosmic rays, which affect a single slit position and detector readout which appears exactly horizontal in this coordinate system. The rest of the features are all consistent with auroral emission matching Cameron band emission.

We compared the locations of the auroral emissions with a statistical model of the Mars crustal magnetic field topology appropriate for the locations of the observations (Figure 4, bottom). We used the map from *Brain et al*. [2007] that shows the probability of open and closed magnetic field lines, based on Mars Global Surveyor measurements of electron pitch angle distributions at 400 km altitude. (Whether or not a particular geographic location is associated with an open or closed field line at any time or altitude depends on many factors, especially solar wind properties and Mars' orientation relative to the Mars-Sun line.) We transform the magnetic field map into the observational coordinate system, with the magnetic field topology pulled from the geographic footprint of each slit pointing at the instant of observation, allowing for slit motion, Mars' rotation, and spacecraft motion. We neglect the ~15 km (sub-pixel) maximum error between the planetodetic coordinate system of the observations and the planetocentric coordinate system of the topology map.

Figure 4 shows that all aurora emissions lie in or near regions with high probabilities of open field lines. Auroral emissions B, C, D, H, I, and L appear against Mars' disk on dark regions of the map. Auroral emissions A and P do lie in regions of open crustal fields, but also lie so close to the limb that their brightness could be attributed to limb enhancement instead. We count these two as inconclusive. Emissions K and M lie very close to statistically open field line regions, and further analysis may show them to be open under the exact magnetic field configuration, altitude and solar wind at the time of the observations. All in all,

the geographic locations of the observed features are consistent with the criteria for discrete aurora as originally observed by Mars Express/SPICAM.

The detection of discrete auroral emission features linked to crustal fields on Orbit 5738 is not an accident of favorable observing geometry. Several images with aurora visible at the limb offered favorable viewing of crustal magnetic fields but presented no statistically significant emission features that might be correlated with regions of open field lines. There is also no indication in the MAVEN/SEP data of changes in the precipitating particles over their entire energy ranges during this orbit. Although there is no specific trigger for so many discrete auroral emission features to occur on this orbit, the occurrence during the event's declining phase is consistent with the correlation pointed by out Brain *et al.* (2006) that local conditions for discrete aurora occur most often when the plasma environment as a whole is already disturbed.

4. Conclusions

The opportunity to measure Mars' diffuse aurora at its strongest recorded levels strengthens the conclusion that the phenomenon must be global in scope. While the IUVS limb scans used in the discovery of diffuse aurora demonstrated that the phenomenon occurred wherever observations were obtained, the finite set of viewing geometries prevented a stronger conclusion about the spatial scale of the aurora. Images such as Figure 1 support the global nature, with relatively uniform emission around the limb and across the disk. Inlimb/outlimb measurements, sampling the region 90 degrees away from the image limb, measured brightnesses comparable to the image limb. The image and limb scan brightnesses in Figure 3 approximately tracked each other, meaning that the global brightness varied approximately in phase around the planet.

The global nature of diffuse aurora is not surprising, given Mars' lack of a dynamo magnetic field, but these observations have provided the strongest evidence to date. We note that IUVS observations cannot prove that emission occurred on the small portion of nightside not visible to MAVEN, nor that aurora occurred on the dayside. The high energies of the particles and the weakness of crustal magnetic fields, however, make both likely. Ironically, the nightside aurora were so intense that IUVS could have detected the emission on the dayside if it did not occur so low in the atmosphere.

The combined auroral and energetic particle observations do not clearly distinguish between electron or proton precipitation as the cause. The particle fluxes, energies and energy fluxes are comparable within about an order of magnitude, so neither can be ruled out based on ability to created bright aurora. Protons and electrons of sufficient energy can reach Mars' nightside: high energy electrons are known to penetrate Mars' nightside to the observed altitudes in previous diffuse aurora observations when high energy protons were absent [Schneider *et al*. 2015a], and the large gyroradius for energetic protons means they too can reach Mars' nightside [*Lillis et al.*, 2016; *Luhmann et al.*, 2007]. Further modelling work on particle trajectories, energy deposition and emission physics is required to resolve the ambiguity, though efforts are hampered by the lack of relevant cross-sections for electron and proton impact ionization and excitation at such high energies.

The event provided two new insights into the role of Mars crustal magnetic fields during space weather events. First, the imprint of crustal magnetic fields during Orbit 5738 shows they do play a role under certain circumstances. The data in hand, though, do not distinguish between two possible end-member sources of precipitating particles: low-energy electrons accelerated by field-aligned potentials, as for discrete aurora [*Brain et al.*, 2006], or some type of crustal field control of the high-energy electrons responsible for the diffuse aurora. (Note that high-energy protons are not a likely source as gyroradii are larger than the

observed features for energies above ~10 keV.) Further observations studies may glean either spectral or altitude information which could narrow down the possible energy range. Modeling of precipitation could give insights in the control of energetic electrons by crustal fields. Second, the lack of wisps and patches during the brightest aurora, when crustal fields were also present in the image frame, suggests that the dominant precipitating particles responsible for the aurora are not diverted or deflected to a significant degree. A future study will examine more closely whether small variations in emissions in other orbits with bright aurora might be associated with crustal magnetic fields. MAVEN's studies of space weather at Mars should improve after the upcoming solar minimum.

Acknowledgments: The MAVEN mission is supported by NASA in association with the University of Colorado and NASA's Goddard Space Flight Center. The authors thank Jean-Claude Gerard for useful discussions. The data may be obtained from the Planetary Atmospheres Node of the Planetary Data System using the filenames and version numbers in the text.

References

Bertaux, J.-L., F. Leblanc, O. Witasse, E. Quemerais, J. Lilensten, S. A. Stern, B. Sandel and O. Korablev (2005), Discovery of an aurora on Mars, *Nature, 435*, 790-794, doi:10.1038/nature03603.

Brain, D. A., J. S. Halekas, L. M. Peticolas, R. P. Lin, J. G. Luhmann, D. L. Mitchell, G. T. Delory, S. W. Bougher, M. H. Acuña, and H. Rème (2006), On the origin of aurorae on Mars, *Geophys. Res. Lett., 33(1)*, 01201, doi:10.1029/2005GL024782.

Brain, D. A., R. J. Lillis, D. L. Mitchell, J. S. Halekas, and R. P. Lin (2007), Electron pitch angle distributions as indicators of magnetic field topology near Mars, *J. Geophys. Res., 112*, A09201, doi:10.1029/2007JA012435.

Deighan, J., S. K. Jain, M. S. Chaffin, X. Fang, J. S. Halekas, J. T. Clarke, N. M. Schneider, A. I. F. Stewart, J.-Y. Chaufray, J. S. Evans, M. H. Stevens, M. Mayyasi, A. Stiepen, M. Crismani, W. E. McClintock, G. M. Holsclaw, D. Y. Lo, F. Montmessin, F. Lefevre, B. M. Jakosky (2018), Discovery of Proton Aurora at Mars, submitted to Nature Astronomy.

Gérard, J. C., Soret, L., Shematovich, V. I., Bisikalo, D. V., & Bougher, S. W. (2017), The Mars diffuse aurora: A model of ultraviolet and visible emissions, *Icarus, 288*, 284-294. DOI: 10.1016/j.icarus.2017.01.037

Gérard, J.-C., *et al.* (2015), Concurrent observations of ultraviolet aurora and energetic electron precipitation with Mars Express, *J. Geophys. Res. 120*, 6749–6765. doi: 10.1002/ 2015JA021150.

Halekas, J. S. (2017), Seasonal variability of the hydrogen exosphere of Mars, *J. Geophys. Res. 122*, 901–911.

Jakosky, B., et al. (2014), The 2013 Mars Atmosphere and Volatile Evolution (MAVEN) mission to Mars, *Space Sci. Rev. 195*, 3–48, DOI: 10.1007/s11214-015-0139-x.

Jakosky, B.M., et al. (2015), MAVEN observations of the response of Mars to an interplanetary coronal mass ejection, *Science 350* (6261).

Larson, D,E. *et al.* (2015), The MAVEN Solar Energetic Particle Investigation, *Space Sci. Rev.* 195,153–172, DOI 10.1007/s11214-015-0218-z.

Lillis, R. J., C. O. Lee, D. Larson, J. G. Luhmann, J. S. Halekas, J. E. P. Connerney, and B. M. Jakosky (2016), Shadowing and anisotropy of solar energetic ions at Mars measured by MAVEN during the March 2015 solar storm, *Journal of Geophysical Research-Space Physics*, *121*(4), 2818-2829, doi:10.1002/2015ja022327.

Luhmann, J. G., C. Zeitlin, R. Turner, D. A. Brain, G. Delory, J. G. Lyon, and W. Boynton (2007), Solar energetic particles in near-Mars space, *J. Geophys. Res. 112*(E10), doi:10.1029/2006je002886.

McClintock, W. E., N.M. Schneider, G.M. Holsclaw, A.C. Hoskins, I. Stewart, J. Deighan, J.T. Clarke, F. Montmessin, R.V. Yelle (2015), The Imaging Ultraviolet Spectrograph (IUVS) for the MAVEN Mission, *Space Sci. Rev*., DOI 10.1007/s11214-014-0098-7.

Ritter, B., Gérard, J.-C., Hubert, B., Rodriguez, L., & Montmessin, F. (2018). Observations of the proton aurora on Mars with SPICAM on board Mars Express, *Geophys. Res. Lett.*, *45*, 612–619. https://doi.org/10.1002/2017GL076235

Schneider, N.M., J. I. Deighan, S. K. Jain, A. Stiepen, A. I. F. Stewart, D. Larson, D. L. Mitchell, C. Mazelle, C. O. Lee, R. J. Lillis, J. S. Evans, D. Brain, M. H. Stevens, W. E. McClintock, M. S. Chaffin, M. Crismani, G. M. Holsclaw, F. Lefevre, D. Y. Lo, J. T. Clarke, F. Montmessin, B. M. Jakosky (2015a); Discovery of diffuse aurora on Mars, *Science 350*, DOI: 10.1126/science.aad0313.

Schneider, N. M., J. I. Deighan, A. I. F. Stewart, W. E. McClintock, S. K. Jain, M. S. Chaffin, A. Stiepen, M. Crismani, J. M. C. Plane, J. D. Carrillo-Sánchez, J. S. Evans, M. H. Stevens, R. V. Yelle, J. T. Clarke, G. M. Holsclaw, F. Montmessin, B.

M. Jakosky (2015b), MAVEN IUVS observations of the aftermath of the Comet Siding Spring meteor shower on Mars, *Geophys. Res. Lett., 42*, 4755–4761, DOI:10.1002/2015GL063863.

Stevens, M.H, J. S. Evans, N. M. Schneider, A. I. F. Stewart, J. Deighan, S. K. Jain, M. Crismani, A. Stiepen, M. S. Chaffin, W. E. McClintock, G. M. Holsclaw, F. Lefèvre, D. Y. Lo, J. T. Clarke, F. Montmessin, S. W. Bougher, B. M. Jakosky (2015), New observations of molecular nitrogen in the Martian upper atmosphere by IUVS on MAVEN, *Geophys. Res. Lett., 42*, DOI: 10.1002/2015GL065319.

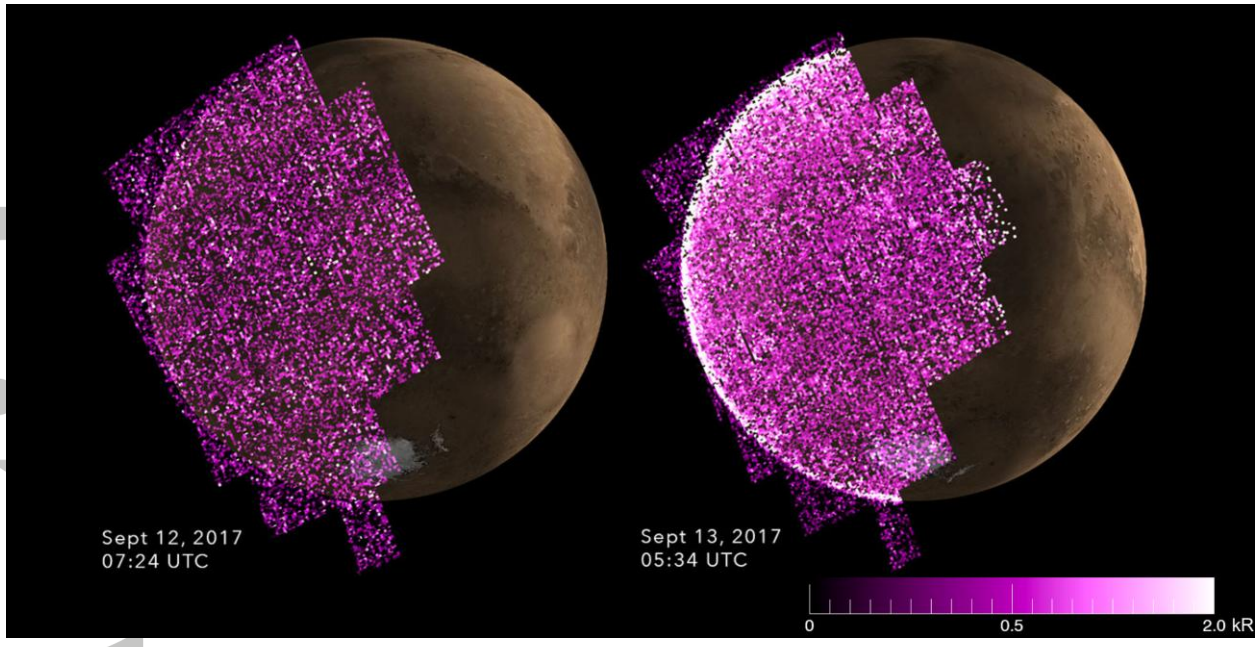

Figure 1. Mid-ultraviolet images of Mars at the start (left) and peak (right) of the September 2017 space weather event. The purple-to-white brightness scale displays the brightness of emission matching the template for CO Cameron bands excited by particle precipitation, spanning the range 0-2.0 kR. The images were obtained on orbits 5726 and 5731 during MAVEN's apoapse orbit segments. IUVS scanned its slit across Mars in six swaths from left to right, while the spacecraft traveled around Mars from top to bottom. In the right image, emission is enhanced across the entire disk, and especially around the limb where projection effects amplify the brightness. In the left image, the limb enhancement is barely visible, and the brightness of the disk is consistent with instrument noise and background. Auroral images were mapped onto the geographic coordinate system of the observation midpoint. Underlying the auroral images are simulated Mars views for the midpoints of the observations, with north up. The day/night terminator is evident across the right side, and the south polar cap at the bottom. Auroral detections were not possible on or near the illuminated crescent.

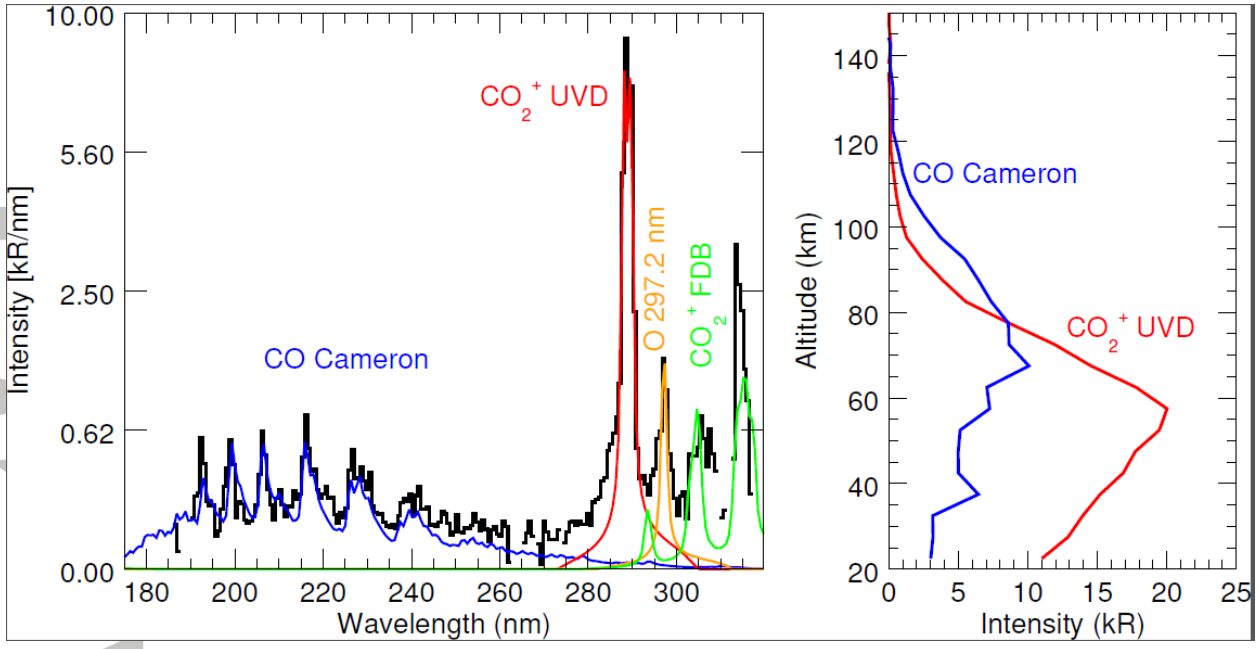

Figure 2. Left: Limb scan spectrum of the brightest auroral emission during orbit 5730, peaking at 60 km altitude. The data are shown in black, with templates for known molecular emissions scaled to match. The plot uses square root scaling to show detail in fainter emissions. Right: Vertical profiles of auroral emissions obtained from the same data, plotting the integrated intensity of the brightest two emissions vs. altitude. The ultraviolet doublet (UVD) shows a sharp peak at 60km altitude, while the CO Cameron bands shows a broader peak around 70 km. The UVD profile primarily reveals the profile of molecular excitation through particle precipitation. In contrast, the Cameron band profile is strongly affected at low altitudes by de-excitation through collisional quenching. Note that dayglow, driven by the absorption of solar EUV radiation, occurs much higher at altitudes around 130 km.

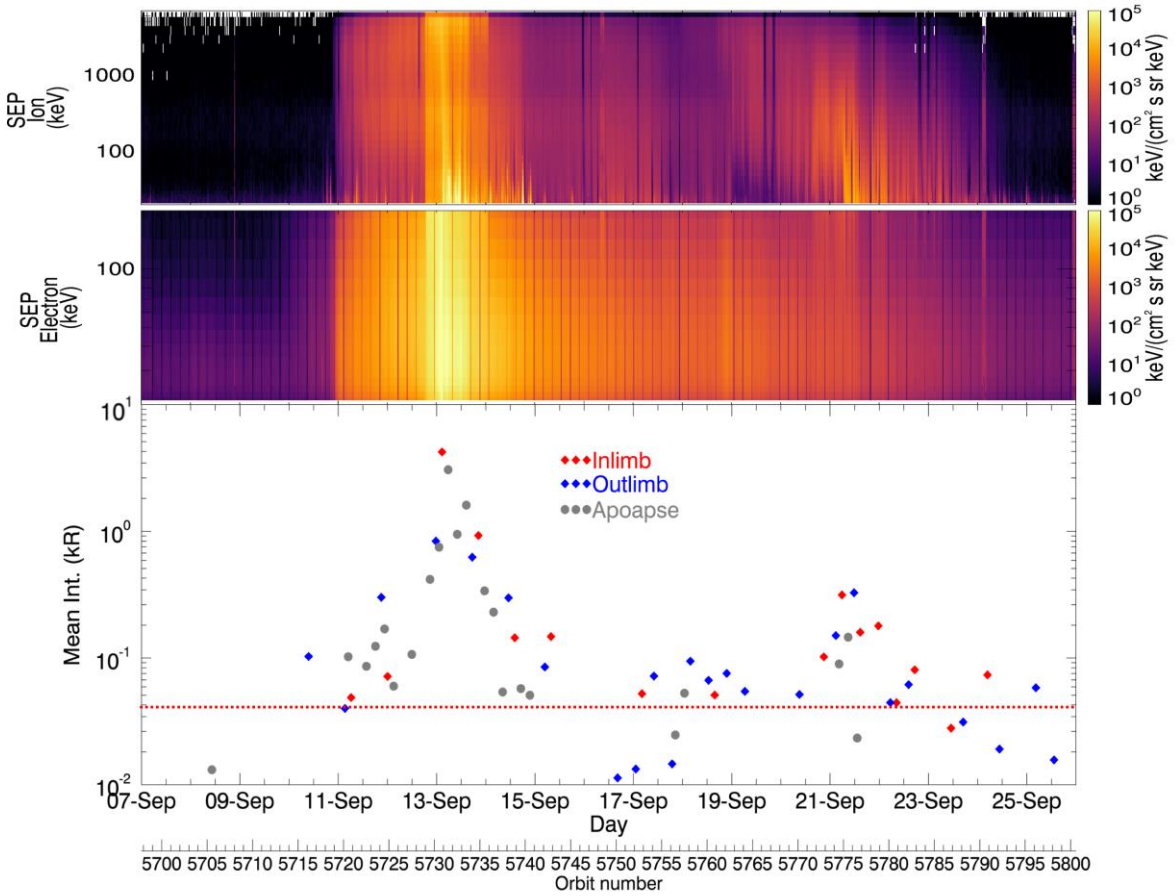

Figure 3. Timeline for auroral emissions and MAVEN/SEP particle fluxes. The bottom panel shows auroral emission from CO Cameron bands in kiloRayleighs. Grey circles show brightnesses in the limb region averaged over 50-100 km extracted from apoapse images as in Figure 1. Red and blue diamonds show the brightness average of the same altitude range in limb scans across the emitting layer obtained about an hour before and after the apoapse images. Limb scans sampled the region roughly at the center of the disk seen in the apoapse images. The red line shows the instrument noise floor which sets a minimum detectable brightness of about 50 R. The timeline shows three auroral episodes, with the brightest one around 13 September at least ten times brighter than the others. The top panels show MAVEN/SEP data, taken from Lee *et al.*, this issue, which are discussed in the text.

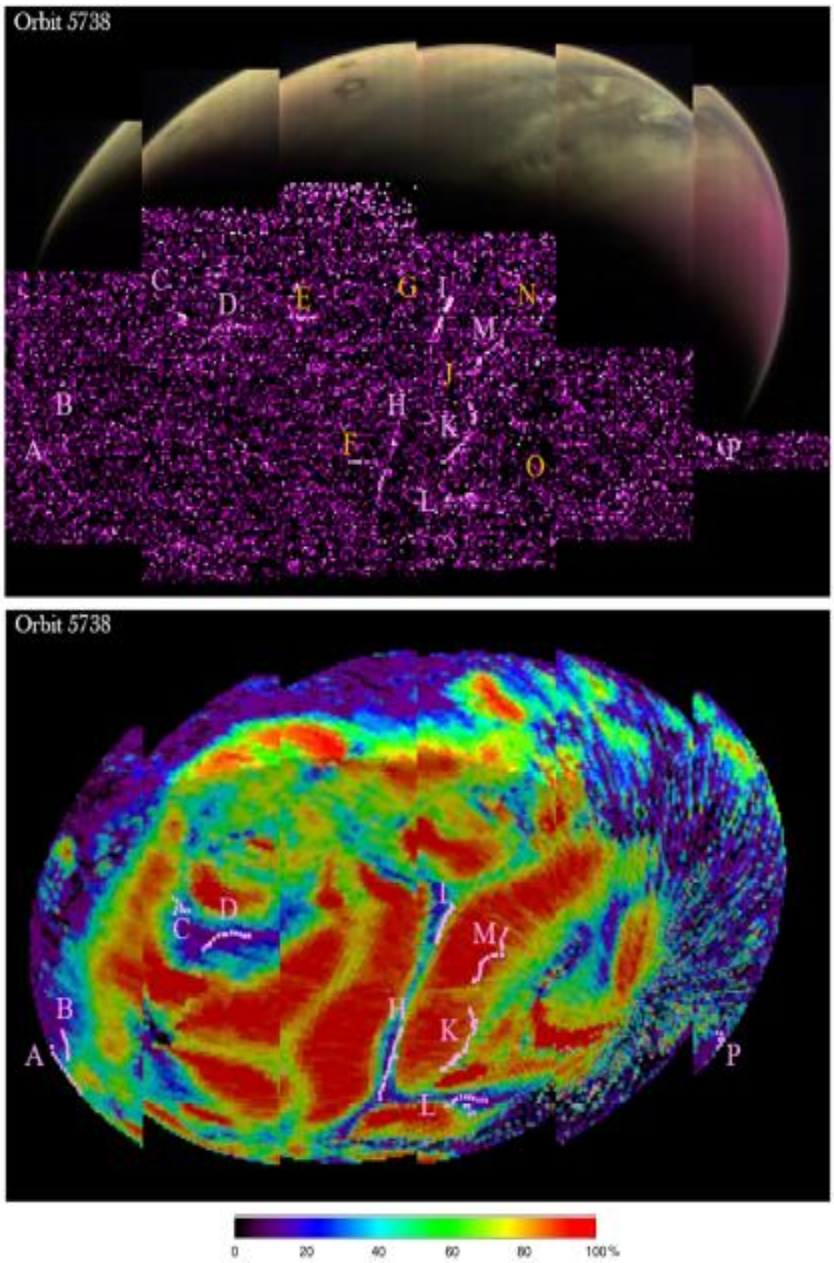

Figure 4. (top) Apoapse image of Mars from orbit 5738, preserving the six vertical swaths of the raw data format. The top portion shows the daylit side with mid-UV colors mapped up to visible colors. North is to the left. The bottom portion of the data image shows the nightside imaged at high gain, using the same purple-white colorbar as Figure 1. Letters identify the locations of wisps and patches of emission analyzed in detail; letters are shown in purple if spectral analysis confirms the auroral nature of the emission, and in orange if spectral analysis indicated an instrumental artifact. (Bottom) The specific pixels in wisps and patches with confirmed auroral spectra are shown in purple with their identifying letter. Features

identified as artifacts in the top panel are omitted from the bottom. The pixels are overplotted on Mars' crustal magnetic field topology from Brain *et al*. (2007) mapped into the observation coordinate system at the moment of each exposure. Red indicates a high probability of closed magnetic field lines, and dark blue indicates a high probability of open field lines.